

# Cholinergic brainstem neurons modulate cortical gamma activity during slow oscillations

Juan Mena-Segovia, Hana M. Sims, Peter J. Magill and J. Paul Bolam

Medical Research Council Anatomical Neuropharmacology Unit, University of Oxford, Mansfield Road, Oxford OX1 3TH, UK

Cholinergic neurons in the rostral brainstem, including the pedunculopontine nucleus (PPN), are critical for switching behavioural state from sleep to wakefulness, and their presumed inactivity during sleep is thought to promote slow cortical rhythms that are characteristic of this state. However, it is possible that the diminished activity of cholinergic brainstem neurons during slow-wave sleep continues to have a functional impact upon ongoing cortical activity. Here we show that *identified* cholinergic projection neurons in the PPN fire rhythmically during cortical slow oscillations, and predominantly discharge in time with the phase of the slow oscillations supporting nested gamma oscillations (30–60 Hz). In contrast, PPN non-cholinergic neurons that are linked to cortical activity fire in the opposite phase and independent of nested gamma oscillations. Furthermore, cholinergic PPN neurons emit extensive local axon collaterals (as well as long-range projections), and increasing cholinergic tone within the PPN enhances the nested gamma oscillations without producing sustained cortical activation. Thus, in addition to driving global state transitions in the cortex, cholinergic PPN neurons *also* play an active role in organizing cortical activity during slow-wave sleep. Our results suggest that the role of the PPN in sleep homeostasis is more diverse than previously conceived. The functions supported by nested gamma oscillations during sleep (i.e. consolidation, plasticity) are critically dependent on the gating of the underlying cortical ensembles, and our data show that cholinergic PPN neurons have an hitherto unappreciated influence on this gating process.

(Received 17 March 2008; accepted after revision 21 April 2008; first published online 25 April 2008)

**Corresponding author** J. Mena-Segovia: Medical Research Council Anatomical Neuropharmacology Unit, University of Oxford, Mansfield Road, Oxford OX1 3TH, UK. Email: [juan.mena-segovia@pharm.ox.ac.uk](mailto:juan.mena-segovia@pharm.ox.ac.uk)

Network oscillations provide a mechanism to functionally link ensembles of neurons. They are likely to be important for information processing, and their dynamic transitions are usually associated with alternations between different brain states (Steriade, 2006). Slow oscillations (~1 Hz), for instance, reflect a highly synchronized activity of large ensembles of neurons across the entire cortex and many subcortical structures, and are present during natural sleep, or can be induced by some anaesthetics (Steriade *et al.* 1990). In contrast, during wakefulness, the slow oscillations are replaced by high-frequency heterogeneous activities whose power and frequency are intimately related to behaviour (Buzsaki & Draguhn, 2004). The transitions from sleep to wakefulness ('waking' the brain) are critically dependent on a group of upper brainstem nuclei that together constitute what has been referred to as the ascending reticular activating system (ARAS). Among the most important components of the ARAS is the pedunculopontine tegmental nucleus (PPN), which is classically considered as a group of cholinergic neurons, but also contains populations of non-cholinergic neurons

(Winn, 2006). Thus, classic experiments have shown that stimulation of fibres in the vicinity of the PPN evokes a shift of sleep to the waking state (Moruzzi & Magoun, 1949), accompanied by the obliteration of slow oscillations and an increase in gamma oscillations (30–60 Hz) in cortex (Steriade *et al.* 1991, 1996; Munk *et al.* 1996). Consistent with this idea, *presumed* cholinergic neurons from the upper brainstem (including PPN) dramatically increase their activities upon waking and arousal, and have been proposed to be actively inhibited in order to promote slow oscillations in the cortex, and consequently sleep (Steriade *et al.* 1990; Saper *et al.* 2005).

Despite most of the established concepts of the basic mechanisms of sleep, emerging evidence shows that sleep and wakefulness are not two opposite or mutually exclusive brain states. Gamma oscillations, usually associated with waking functions (e.g. environmental information processing and learning), are present (nested) during the slow oscillations in the deeper stages of sleep (Steriade, 2006); their emergence is associated with the depolarization of cortical neurons, which occurs in the

phase referred as the active component of the slow oscillation, or 'up' state (i.e. at the peak of the oscillation). The network dynamics during 'up' states have been proposed to be equivalent to those observed during the waking state, and consequently some of the cognitive functions that underlie this activity (Destexhe *et al.* 2007). Both gamma oscillations and 'up' states have been shown to occur also in functional isolation (e.g. in a brain slice), suggesting that the intrinsic cortical circuits are enough to provide at least a basal level of this activity (Llinas *et al.* 1991; Whittington *et al.* 1995; Sanchez-Vives & McCormick, 2000). Yet, the coherence of *nested* gamma oscillations between distant cortical areas observed during experimental conditions suggests that local cortical circuits might not be enough to generate intracortical synchronization (Molle *et al.* 2004). Thus, it is possible that subcortical structures also contribute to the highly synchronized activity characteristic of the 'up' state.

Modulation of the cortical gamma activity by subcortical structures has been observed only during the waking state. During sleep, there is no direct evidence that relates subcortical activity to global brain activity, although there is some suggestion that low levels of activity remain in wake-inducing structures (Steriade *et al.* 1990; Lee *et al.* 2005). It is therefore possible that, in the intact brain, the cortical network dynamics during 'up' states are *also* modulated by subcortical afferents, including those engaged by the ARAS. To address this issue, we used a highly selective method for recording and labelling individual neurons *in vivo* in the PPN and relating their activity to ongoing global activity. We present data on firing properties and connectivity of identified cholinergic neurons, and we propose, on the basis of their physiological and anatomical properties, and on the basis of pharmacological manipulations, that they contribute to the ongoing cortical activity during slow oscillations.

## Methods

### Electrophysiological recordings, juxtacellular labelling and local drug application

Experiments were carried out on 53 adult male Sprague-Dawley rats (250–310 g; Charles River, Margate, UK) in accordance with the Animals (Scientific Procedures) Act, 1986 (UK). Anaesthesia was induced with 4% v/v isoflurane in O<sub>2</sub>, and maintained with urethane (1.3 g kg<sup>-1</sup>, i.p.), and supplemental doses of ketamine (30 mg kg<sup>-1</sup>, i.p.) and xylazine (3 mg kg<sup>-1</sup>, i.p.), as previously described (Magill *et al.* 2004). Electrocardiographic (ECG) activity, respiration rate, the electrocorticogram (ECoG; described below) and reflexes were monitored to ensure the animals' well-being and depth of anaesthesia.

The ECoG was recorded via a 1 mm diameter steel screw juxtaposed to the dura mater above the frontal cortex

(2.7 mm anterior and 2.0 mm lateral of bregma; Paxinos & Watson, 1986), which corresponds to the somatic sensorimotor cortex (Donoghue & Wise, 1982).

Extracellular recordings of action potentials of PPN neurons were made using 15–25 M $\Omega$  glass electrodes (tip diameter  $\sim$ 1.5  $\mu$ m), which contained saline solution (0.5 M NaCl) and neurobiotin (1.5% w/v, Vector Laboratories, Peterborough, UK). Electrode signals were amplified (10 $\times$ ) through the active bridge circuitry of an Axoprobe-1A amplifier (Molecular Devices Corp., Sunnyvale, CA, USA), AC-coupled and amplified a further 100 $\times$  (NL-106 AC-DC Amp: Digitimer Ltd, Welwyn Garden City, UK), before being band-pass filtered between 0.3 and 5 kHz (NL125: Digitimer). All biopotentials were digitized on-line with a PC running Spike2 acquisition and analysis software (version 5; Cambridge Electronic Design, Cambridge, UK). To neurochemically and morphologically characterize the recorded units, neurons were then labelled with the neurobiotin by the juxtacellular method (Pinault, 1996; Magill *et al.* 2000; Ungless *et al.* 2004).

Activity was recorded, first, during slow-wave activity, which accompanies deep anaesthesia and is similar to activity observed during natural sleep, and second, during episodes of spontaneous or sensory-evoked 'global activation', which contain patterns of activity that are more analogous to those observed during the awake, behaving state (see review by Steriade, 2000). Sensory stimulation and subsequent global activation were elicited by a standard pinch of the hindpaw as previously described (Magill *et al.* 2004). The animals did not respond overtly to the pinch.

Extracellular recordings of local field potentials (LFPs) and multi-unit activity in the PPN were made using 'silicon probes' (model number 1 cm 100–400; NeuroNexus Technologies, Ann Arbor, MI, USA). Each probe had 16 recording contacts arranged in a single vertical plane, with a contact separation of 100  $\mu$ m. Each contact had an impedance of 0.9–1.3 M $\Omega$  (measured at 1000 Hz) and an area of  $\sim$ 400  $\mu$ m<sup>2</sup>. Monopolar signals recorded using the probes were referenced against a screw implanted in the skull above the contralateral cerebellar hemisphere. Probes were advanced into the brain under stereotaxic control (Paxinos & Watson, 1986), at an angle of 15 degrees to the vertical to avoid prominent blood vessels. Probes were advanced slowly using a zero-drift micromanipulator (1760-61; David Kopf Instruments), and large blood vessels (greater than  $\sim$ 50  $\mu$ m diameter) lying on the cortical surface were avoided. This approach ensured that dimpling of the cortex was avoided and that no gross deformation or bending of the probe occurred. The latter is borne out by the straight tracks that were seen in the tissue after histological processing (see below). Extracellular signals from the silicon probe were amplified (1000–2000 $\times$ ) and

low-pass filtered (0–6000 Hz) using computer-controlled differential amplifiers (Lynx-8; Neuralynx, Tucson, AZ, USA). The ECoG and probe signals were each sampled at 17.5 kHz. The ECG and respiration signals were sampled at 400 and 64 Hz, respectively. All biopotentials were digitized on-line using a Power1401 analog-to-digital converter (Cambridge Electronic Design) and a personal computer running Spike2 acquisition and analysis software (version 5; Cambridge Electronic Design). Recording locations were verified using histological procedures described below.

For local drug application, glass pipettes (tip diameter 20–40  $\mu\text{m}$ ) were filled with saline solution (0.9% w/v NaCl) containing an acetylcholine receptor agonist, carbachol (20 mM), or saline alone, and inserted into the brain under stereotaxic control. Small volumes were slowly infused (100 nl over 30 s, total dose: 2 nmol) and their effects on the frequency and power of ipsilateral and contralateral ECoG activity were quantified (see below). A higher dose was also used to test the effect on global activation (500 nl of 200 mM carbachol, total dose: 100 nmol). Locations of drug application pipettes were verified using standard histological procedures.

### Histochemistry and immunocytochemistry

The neurochemical identities of juxtacellularly labelled neurons were verified using standard immunofluorescence

and histofluorescence techniques (see Fig. 1; Ungless *et al.* 2004). The neurobiotin was revealed by incubating tissue sections (60  $\mu\text{m}$ ) in CY3-conjugated to streptavidin (1:1000, Jackson ImmunoResearch Laboratories, Inc., USA). The presence of choline acetyltransferase (ChAT), the synthetic enzyme for acetylcholine, was revealed by incubation in goat anti-ChAT antibodies (1:500, Chemicon, USA) followed by Alexa 488 conjugated to donkey anti-goat antibodies (1:1000, Jackson). Sections were then mounted on slides for viewing with a conventional epifluorescence microscope (DMRB: Leica Microsystems GmbH, Wetzlar, Germany) or a laser-scanning confocal fluorescence microscope (LSM510: Karl Zeiss AG, Oberkochen, Germany).

Following neurochemical identification, standard histochemical techniques were used to visualize cells with a permanent peroxidase reaction product for light and electron microscopic analyses (Kita & Armstrong, 1991; Pinault, 1996; Ungless *et al.* 2004). Sections were dehydrated and mounted in resin for light and electron microscopy as previously described in detail (Bevan *et al.* 1998). Following light microscopic analysis, areas of interest were re-embedded in blocks of resin, sectioned on an ultramicrotome (Leica) and examined in a Philips CM100 or CM10 electron microscope.

The somatodendritic and axonal arborizations of neurobiotin-labelled, PPN neurons were reconstructed from successive serial sections (60  $\mu\text{m}$ )

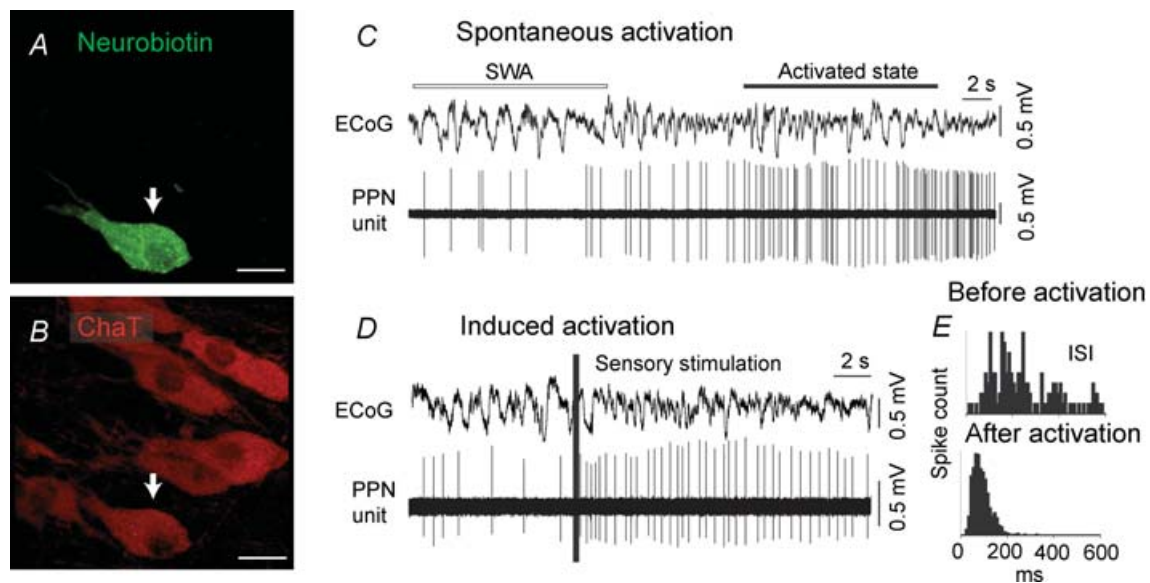


**Figure 1. Identified cholinergic PPN neurons increase their activity during transitions from slow oscillations to global activation**

*A* and *B*, PPN neurons were juxtacellularly labelled and identified as cholinergic by the co-localization of fluorescent markers for the neurobiotin and choline acetyltransferase immunoreactivity (arrows). *C*, example of spontaneous activation of a PPN cholinergic neuron during transition from cortical slow oscillations to an activated state. *D*, example of induced activation of a cholinergic neuron. Shortly after the onset of a hindpaw pinch (indicated by the vertical bar; sensory stimulation), cholinergic neurons increased their firing rate and became more regular. *E*, the interspike interval (ISI) shows a more regular pattern during the activated state than before activation. Scale bars in *A* and *B*: 20  $\mu\text{m}$ .

using a  $63\times$  objective, and were digitized using NeuroLucida software (MicroBrightField, Williston, VT, USA).

### Electrophysiological data analysis

Data from the recording sessions were visually inspected and epochs of robust cortical slow wave activity (SWA) were identified (Magill *et al.* 2000). Gamma oscillations were extracted from the wideband ECoG by off-line digital filtering between 30 and 50 Hz (Finite Impulse Response filters: Spike2). The Lomb algorithm was used to determine the statistical significance and frequency of any periodic discharge features (within the 0.5–50 Hz range) present in the spike train (Kaneoke & Vitek, 1996). Frequency spectra of spiking are displayed as ‘Lomb periodograms’. The relative power of a peak in the periodogram is indicated by the clearance of the peak from the significance level of  $P = 0.05$  (represented by dashed lines in Fig. 2D and H).

Temporal relationships between activities in cortex and PPN were estimated from spike-triggered waveform averages of the coincident ECoG (Spike2) and phase histograms. Power spectra of the ECoG were calculated using the Fast Fourier Transform function of Spike2. To determine the phase relationship of the PPN spikes with the different components of the cortical slow oscillations (active *versus* inactive components), the ECoG signal was filtered below 4 Hz to retain slow oscillations and exclude high frequencies to improve the ‘peak’ (active component) and ‘trough’ (inactive component) detection. Slow oscillation periods and peaks-and-troughs were detected automatically using custom MATLAB routines, based on the time of zero crossing and taking into account the average time-width of peaks and troughs (as peaks are longer than troughs). Each spike was assigned to a given phase (bin size 36 deg) between zero crossings and all identified 1 Hz cycles were superimposed.

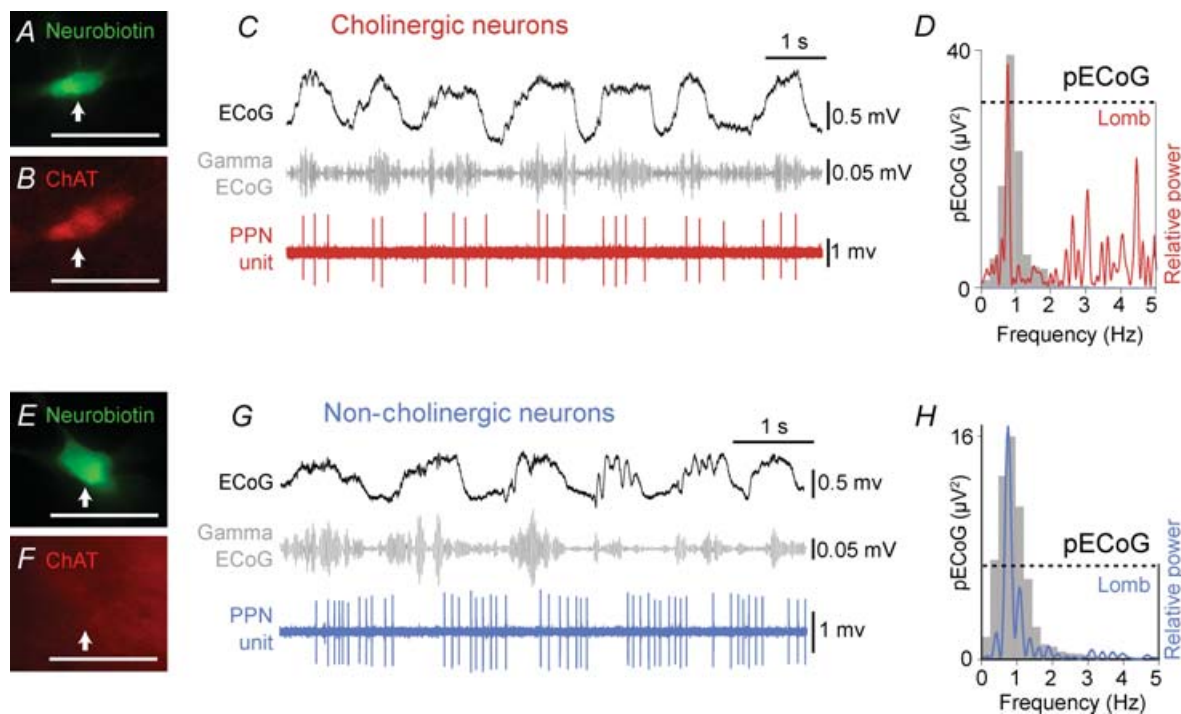


**Figure 2. Cholinergic PPN neurons fire in time with cortical slow-wave activity and nested increases in gamma oscillations**

A and B, a cholinergic PPN neuron was juxtacellularly labelled and identified as such by the co-localization of fluorescent markers for the neurobiotin and choline acetyltransferase immunoreactivity (ChAT; arrows). C, during robust slow-wave activity, cortical activity (ECoG; black) was dominated by a slow oscillation ( $\sim 1$  Hz), the active components of which supported the nested gamma oscillations (30–50 Hz; grey). Cholinergic PPN neurons were active and fired groups of spikes (PPN unit, red) in time with the slow and gamma oscillations. D, power spectra of slow oscillations (grey) in the ECoG (pECoG) and Lomb periodogram (red) of the single cholinergic unit. As shown in the Lomb periodogram, the neuron oscillated at a frequency similar to that of the cortical slow oscillation. E and F, a PPN non-cholinergic neuron was identified as such following the juxtacellular labelling and the lack of co-localization of fluorescent markers for neurobiotin and ChAT (arrows). G, as with cholinergic neurons, non-cholinergic neurons also fired groups of spikes (blue) during robust slow oscillations (black), although their firing was not timed with gamma oscillations (grey). H, the pECoG (grey) and Lomb periodogram (blue) of the single non-cholinergic unit also show a significant peak of oscillation at  $\sim 1$  Hz. Dashed lines in D and H represent the level of significance. Scale bars:  $50 \mu\text{m}$ .

For the visual detection of the effect on gamma oscillations following the drug applications, Spike2 files were imported to MATLAB using SON libraries. ECoG signal was filtered and the slow oscillations detected as described above. The spectrogram was calculated (fft 1024, win 1024, overlap 1008) for the original ECoG signal and trigger-averaged with the times of trough-to-peak transition. The same colour scale was maintained for ipsilateral and contralateral for comparison purposes. The Wilcoxon Signed Rank test was used to compare paired data. The significance level for all tests was taken to be  $P < 0.05$ . Data are expressed as mean  $\pm$  standard error of the mean (S.E.M.).

## Results

### Slow wave activity (SWA) and activated state

Urethane anaesthesia typically produced SWA characterized by a stable slow oscillation in the cortex that bears a close resemblance to the activity observed during the deeper stages of slow-wave sleep in mammals (see Discussion; Figs 1 and 2). These slow oscillations were defined by their large amplitude ( $> 400 \mu\text{V}$ ) and low frequency ( $\sim 1$  Hz), and their coexistence with higher-frequency activity of smaller amplitude ( $< 200 \mu\text{V}$ ), including gamma oscillations (30–60 Hz; Fig. 2). The portions of the slow oscillation supporting gamma oscillations are analogous to activity during wakefulness, with synchronous spike discharges in cortical neurons and other similarities in network dynamics (Steriade, 2006; Destexhe *et al.* 2007; Rudolph *et al.* 2007), and will be referred to hereafter as the ‘active component’. The portions during which high-frequency oscillations are weakest, or absent, will thus be referred to as the ‘inactive component’. This terminology is used in preference to ‘up’ and ‘down’ states as these generally refer to membrane states of individual neurons as recorded intracellularly.

SWA was spontaneously interspersed with periods of cortical activation (also referred to as the *activated state*), defined by a progressive disappearance of slow oscillations that was replaced by a sustained ( $> 3$  s) period of low amplitude ( $< 200 \mu\text{V}$ ) and fast frequency ( $> 5$  Hz) heterogeneous activity. Cortical activation could also be abruptly induced by sensory stimulation (see Methods). The response time of the cortex to switch from SWA to an activated state following sensory stimulation varied between animals and conditions, and was particularly dependent on the depth of anaesthesia.

### Identified cholinergic neurons modulate transitions of global brain-states

We recorded the action potential discharges of single PPN neurons and related them to ongoing cortical oscillations in anaesthetized rats. After electrophysiological

characterization, 102 of the 159 recorded PPN neurons were labelled *in vivo* by the juxtacellular method. Of those neurons, 36 were examined by immunofluorescence and 11 of them were identified as cholinergic by the expression of immunoreactivity for choline acetyltransferase (ChAT; Figs 1A and B, and 2A and B). The activity of identified cholinergic neurons was monitored before and during spontaneous or sensory-evoked transitions from slow oscillations to an activated cortical state ( $n = 9$ ). During spontaneous transitions, cholinergic neurons that were already firing at low frequencies began to increase their firing rate while the cortex became activated (Fig. 1C). During the foot-pinch, the same neurons showed a fast, significant increase in their firing rate (Fig. 1D; rate during SWA =  $11.03 \pm 5.7$  Hz; rate during activation =  $15.1 \pm 6.5$  Hz;  $P < 0.05$ ,  $n = 9$ ) and their firing patterns became more regular (Fig. 1E; mean coefficient of variation (CV) during SWA =  $1.2 \pm 0.18$ ; CV during activation =  $0.6 \pm 0.11$ ,  $n = 9$ ). These results support and extend the notion proposed by Steriade and colleagues (Steriade *et al.* 1990, 1991) that PPN cholinergic projections modulate brain-state and behavioural transitions in that we demonstrate *directly* the involvement of cholinergic neurons in the response to cortical activation.

### Cholinergic neurons are still active during cortical slow-wave activity

The extracellular unit recordings revealed that identified cholinergic PPN neurons (Figs 1A and B, and 2A and B) are still active during robust cortical slow oscillations (Fig. 2C; see also Fig. 1C and D). The activity of all cholinergic neurons that were firing during cortical slow-wave activity ( $n = 9$ ) was organized in groups of spikes following the slow oscillations in the cortex, producing a significant oscillation at a frequency near to 1 Hz (Lomb periodogram; Fig. 2D). This oscillatory pattern fades away during periods of absence of slow oscillations in the cortex (two neurons were not considered because the cortex was activated). We identified two subgroups within the cholinergic neuronal population: slow firing neurons ( $n = 6$ ; mean rate =  $0.9 \pm 0.3$  Hz; CV =  $0.95 \pm 0.2$ ) that were temporally correlated with the nested gamma oscillations (Fig. 2C), and fast firing neurons ( $n = 3$ ; mean rate =  $31.3 \pm 8.8$  Hz; CV =  $1.7 \pm 0.12$ ) characterized by their lack of correlation with nested gamma oscillations (not shown).

### The activities of cholinergic and non-cholinergic neurons are different during the slow oscillations

Of the 36 neurons that were recorded, labelled and examined by immunofluorescence, 25 of them were

identified as non-cholinergic by the lack of expression of immunoreactivity for ChAT (Fig. 2E and F). In contrast to the cholinergic neurons, the activity of only about one third of non-cholinergic neurons (8 of 25) was correlated with the activity in the cortex. These neurons fired in groups of spikes (mean rate =  $3.8 \pm 0.88$  Hz; mean CV =  $1.3 \pm 0.7$ ,  $n = 8$ ) and showed a significant oscillation at a frequency of  $\sim 1$  Hz, as with cholinergic neurons, but showed an opposite relationship to the gamma episodes nested within the slow oscillations (Fig. 2G and H).

Two other firing patterns were commonly observed among non-cholinergic neurons: very slow firing (nearly silent) neurons ( $< 0.5$  Hz) and tonically firing neurons. Both subtypes fired independently of the pattern of activity in the cortex and therefore will be the subject of a separate communication.

### Spike timing of PPN neurons relative to cortical slow oscillations

We then analysed the temporal relationship of the spikes of the different subtypes of PPN neurons compared to the activity of the cortex during SWA (Fig. 3). We observed that each neuronal subtype fired in a specific phase of the slow oscillations. The main subtype of cholinergic neurons (6 of 9) fired predominantly during the active component of the slow oscillations (ChATa, *active component-locked*), the firing was thus in phase with the gamma oscillations nested within the slow waves (Fig. 3A). In contrast, non-cholinergic neurons ( $n = 8$ ) fired preferentially during the inactive component, that is, after cholinergic neurons reached their maximal probability of firing (Fig. 3B). The minor subtype of cholinergic neurons (3 of 9) fired also during the inactive component (ChATi, *inactive component-locked*) but after non-cholinergic neurons fired (Fig. 3C). Thus, the maximal probability of firing of non-cholinergic and ChATi neurons occurs when gamma oscillations are almost *absent* in the cortex. As these characteristics of the spike-timing in relation to slow oscillations is constant across recordings and across different animals, we considered the spike timing as a *physiological signature* of the different types of neurons in the PPN that are coupled to cortical activity.

To determine whether the differences in spike-timing of the PPN neuronal subtypes in relation to the cortical slow oscillations occur simultaneously within one recording session, we recorded the activity of multiple PPN neurons using high-density multi-electrode arrays ('silicon probes') during cortical SWA ( $n = 3$ ). Thus, we observed large numbers of neurons firing with different patterns, from which we isolated those whose firing was in time with the cortical slow oscillations. We found the same three patterns of activity described in the juxtacellularly

labelled neurons in the simultaneous probe recordings (Fig. 3D), as shown by their timing in relation to slow oscillations (Fig. 3E). These neurons were identified as putative ChATa neurons ( $n = 6$ ), putative non-cholinergic neurons ( $n = 3$ ), or putative ChATi neurons ( $n = 3$ ), and all of them were oscillating at the same frequency as the slow oscillations in the cortex ( $\sim 1$  Hz; Fig. 3F), although they were coupled to different phases.

### Long range projections of cholinergic neurons

After neurochemical characterization by immunofluorescence, the recorded PPN neurons were processed to reveal the neuronal marker, neurobiotin, with a permanent peroxidase reaction product that enabled us to examine and reconstruct their dendrites and axonal arbors. The labelled neurons were distributed across the rostro-caudal and dorsoventral extents of the PPN (Fig. 4). Morphological properties of the subtypes of PPN neurons are summarized in Table 1.

All the cholinergic neurons that were peroxidase-labelled and traced ( $n = 10$ ) had similar axonal arborizations; the main branch travelled caudally from the cell body and along the trajectory of the superior cerebellar peduncle before dividing into four to six collaterals that ascended towards the forebrain and descended towards the hindbrain (Fig. 5A). Thus, *individual* cholinergic ChATa neurons characteristically innervated, via their extensive collaterals, many of the known target regions of the PPN, including the intralaminar thalamus (central lateral and parafascicular nuclei), superior and inferior colliculi, the basal ganglia (subthalamic nucleus, substantia nigra pars reticulata and pars compacta) and the lower brainstem (with particularly dense projections to the pontine oralis and caudalis nuclei). None of the ChATi neurons were labelled sufficiently well enough to allow the identification of distant targets. These findings are in agreement with previously published retrograde labelling studies showing that cholinergic PPN neurons are projection neurons that innervate many regions of the brain (Garcia-Rill, 1991; Pahapill & Lozano, 2000; Mena-Segovia *et al.* 2004), but our single-cell labelling study shows for the first time that it is *individual* cholinergic neurons that project to multiple targets via their collaterals.

In contrast, peroxidase-labelled non-cholinergic neurons ( $n = 6$ ) showed a different pattern of axonal projections, having a single branch initially directed caudally along the superior cerebellar peduncle fibres, and then turning either dorsally or ventrally, and sometimes giving rise to a second branch travelling in the same direction (Fig. 5B). No descending collaterals were observed in this group. Despite coursing for long distances, axons mainly travelled in the sagittal plane rather than the medio-lateral plane. Three main targets were identified for neurons whose axon was sufficiently

well labelled to enable them to be traced: subthalamic nucleus, substantia nigra pars reticulata and substantia nigra pars compacta. In these targets, several varicosities were identified, some of which were identified by electron microscopy to give rise to asymmetric synapses (not shown).

### Local connectivity of cholinergic neurons

The cholinergic neurons gave rise to extensive local axon collaterals within the PPN. These collaterals were studied with varicosities (Fig. 6; mean number of local varicosities,  $59 \pm 25$ ,  $n = 10$ ), and some were identified by electron

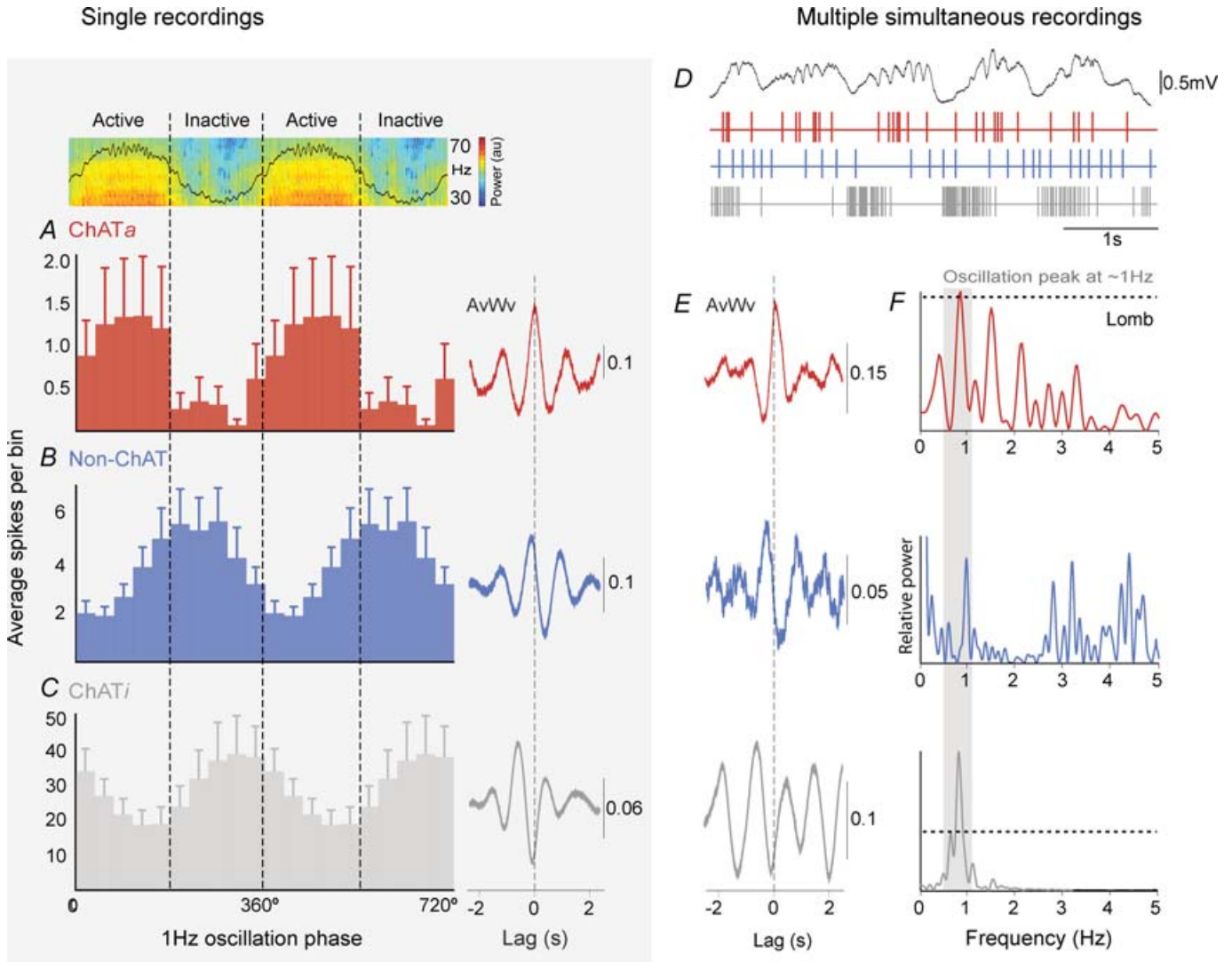


**Figure 3. The firing of the different neuronal subtypes reflects phase selectivity relative to the cortical slow oscillations**

A–C, phase relationships between a typical ECoG (above A) and the activity of PPN neurons (average spikes per bin), and single representative cases of their corresponding spike-triggered averages of ECoG waveforms (right, AvWv). A, most cholinergic PPN neurons fired preferentially during the active component of the slow oscillations and, thus, phasic increases in gamma oscillations ( $n = 6$ ). Large error bars are due to the low firing rate of some of the cholinergic neurons in this group. In contrast, non-cholinergic neurons (B,  $n = 8$ ) and a minority of cholinergic neurons (C,  $n = 3$ ) fired preferentially during the inactive component of the slow oscillation. D, traces from the ECoG and the firing of three different neurons (represented as events) recorded simultaneously using high-density multi-electrode arrays. E, the representative spike-triggered averages of ECoG waveforms show the phases of the cortical slow oscillation in which they preferentially fire, allowing the comparison with the juxtacellularly labelled neurons (left), and thus their identification as putative *active component-locked* cholinergic neurons (ChATa, red), putative non-cholinergic neurons (Non-ChAT, blue) or putative *inactive component-locked* cholinergic neurons (ChATi, grey). F, even though their firing was timed with different components of the slow oscillation, they all show a peak of oscillation at  $\sim 1$  Hz, as shown by the Lomb periodograms (dashed lines in top and bottom panels represent level of significance).

**Table 1. Morphological properties of peroxidase-labelled PPN neurons**

	Cell body area ( $\mu\text{m}^2$ )	Total no. dendritic spines	No. of primary dendrites	Total dendritic length ( $\mu\text{m}$ )	Mean dendritic length ( $\mu\text{m}$ )	No. of local boutons
ChATa neurons ( $n = 6$ )	$378 \pm 60$	$29 \pm 16$	$4.67 \pm 0.36$	$2729 \pm 441$	$595 \pm 62$	$74 \pm 35$
ChATi neurons ( $n = 2$ )	432	0	4	768	228	48
Non-cholinergic neurons ( $n = 6$ )	$162 \pm 33$	$32 \pm 32$	$5.17 \pm 0.6$	$2736 \pm 752$	$633 \pm 201$	$5 \pm 4$

Values shown are mean  $\pm$  s.e.m. for ChATa and non-cholinergic neurons, or only mean for ChATi neurons. Two cholinergic labelled neurons were not included in this table because they could not be classified as either ChATa or ChATi neurons.

microscopy as forming synapses with the dendrites of PPN neurons (Fig. 6B). The axons of non-cholinergic neurons did not give rise to local collaterals and had few, if any, varicosities within the boundaries of the PPN (Fig. 6C). Thus, PPN cholinergic neurons form an extensive local network and *individual* cholinergic neurons are in a position to *simultaneously* influence neighbouring neurons within the PPN *and* neurons in many different regions of the brain.

### Impact of the cholinergic tone within PPN upon cortical gamma oscillations

The PPN is a wake-inducing structure, and increased synaptic drive from its cholinergic neurons has been indirectly associated with the emergence of cortical gamma oscillations during activated or waking brain states (Steriade *et al.* 1991; Munk *et al.* 1996). The temporal relationship between the activity of ChATa neurons and cortical gamma oscillations that we show here suggests, however, that they also have an impact on cortical gamma oscillations during slow oscillations. Cholinergic neurons

have an extensive local axon collateral network (Fig. 6), and this is likely to underlie a cholinergic tone in the PPN. Thus, in order to establish whether a causal link exists between PPN activity and cortical gamma oscillations during SWA, we tested the effects of pharmacological (cholinergic) manipulation of PPN on ongoing cortical activity, as revealed by the frequency and power of ECoGs. Small focal injections into PPN ( $n = 5$  animals) of a nicotinic and muscarinic acetylcholine receptor agonist, carbachol, produced a marked effect exclusively on the active component of the cortical slow oscillations. The power of cortical gamma oscillations (30–50 Hz) significantly increased after the carbachol injection (Fig. 7A–C), but the slow oscillations at  $\sim 1$  Hz were not affected (Fig. 7D). The specificity of this effect for the PPN was demonstrated by the fact that injection of carbachol into the region lateral or dorsal to PPN did not significantly affect cortical gamma oscillations ( $n = 2$  animals). Infusion of a larger dose of carbachol (100 nmol) produced a sustained activation of the ECoG, as shown by the obliteration of the slow oscillations in the cortex (Fig. 7E). Thus, taken together with the spike-timing specificity of cholinergic neurons for the active component, these data suggest that the activity of the cholinergic network in the PPN enhances the expression of ongoing cortical gamma oscillations during slow oscillations through their long-range projections presumably to the thalamus and/or the basal forebrain.

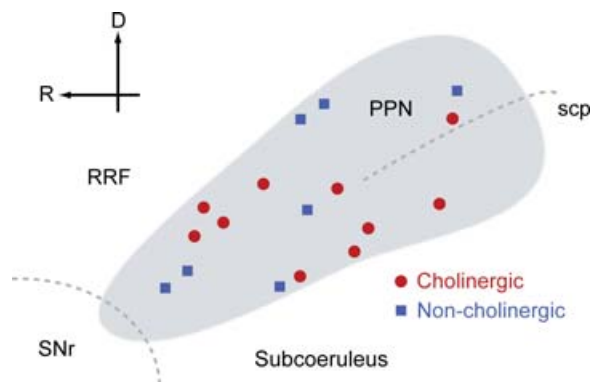


**Figure 4. Schematic representation of the PPN showing the positions of the labelled neurons**

Cholinergic (circles) and non-cholinergic (squares) neurons in the PPN were labelled throughout the rostro-caudal and dorso-ventral extent. The boundaries of the PPN were defined by the presence of immunoreactivity for ChAT. D, dorsal; R, rostral; RRF, retrorubral field; scp, superior cerebellar peduncle; SNr, substantia nigra pars reticulata.

### Discussion

Our findings constitute the first direct evidence that brainstem cholinergic neurons in the PPN are active during the slow oscillations that are prevalent during general anaesthesia and slow-wave sleep. Not only is the activity of cholinergic PPN neurons timed with specific components of the cortical slow oscillations but it also has a clear functional bearing on the gamma oscillations nested therein. Indeed, our data suggest that cholinergic PPN neurons play a hitherto unappreciated role in modulating cortical gamma oscillations during sleep.

The role of the brainstem cholinergic neurons as critical modulators of the sleep–wake cycle was proposed more



than half a century ago (along with the development of the concept of the ARAS), but was first demonstrated by Steriade and colleagues (Steriade *et al.* 1991), who showed that such a mechanism was cholinergic and was mediated through the thalamus. Supporting this evolving concept of activation, our results confirm this close association of cholinergic PPN neurons with global state transitions, and show, for the first time, that *identified* cholinergic neurons increase their firing rate during the process of cortical activation. Having defined the firing characteristics of

identified cholinergic neurons, we then demonstrated that the *same* neurons that modulate brain state transitions fire in a highly organized manner during the cortical slow oscillations in association with the cortical gamma activity nested within the slow oscillations. These properties of PPN cholinergic neurons strongly suggest that they continue to influence activity in the cortex even during slow-wave sleep.

Our findings have equal relevance to anaesthesia and to the natural sleep state. The validation of the use

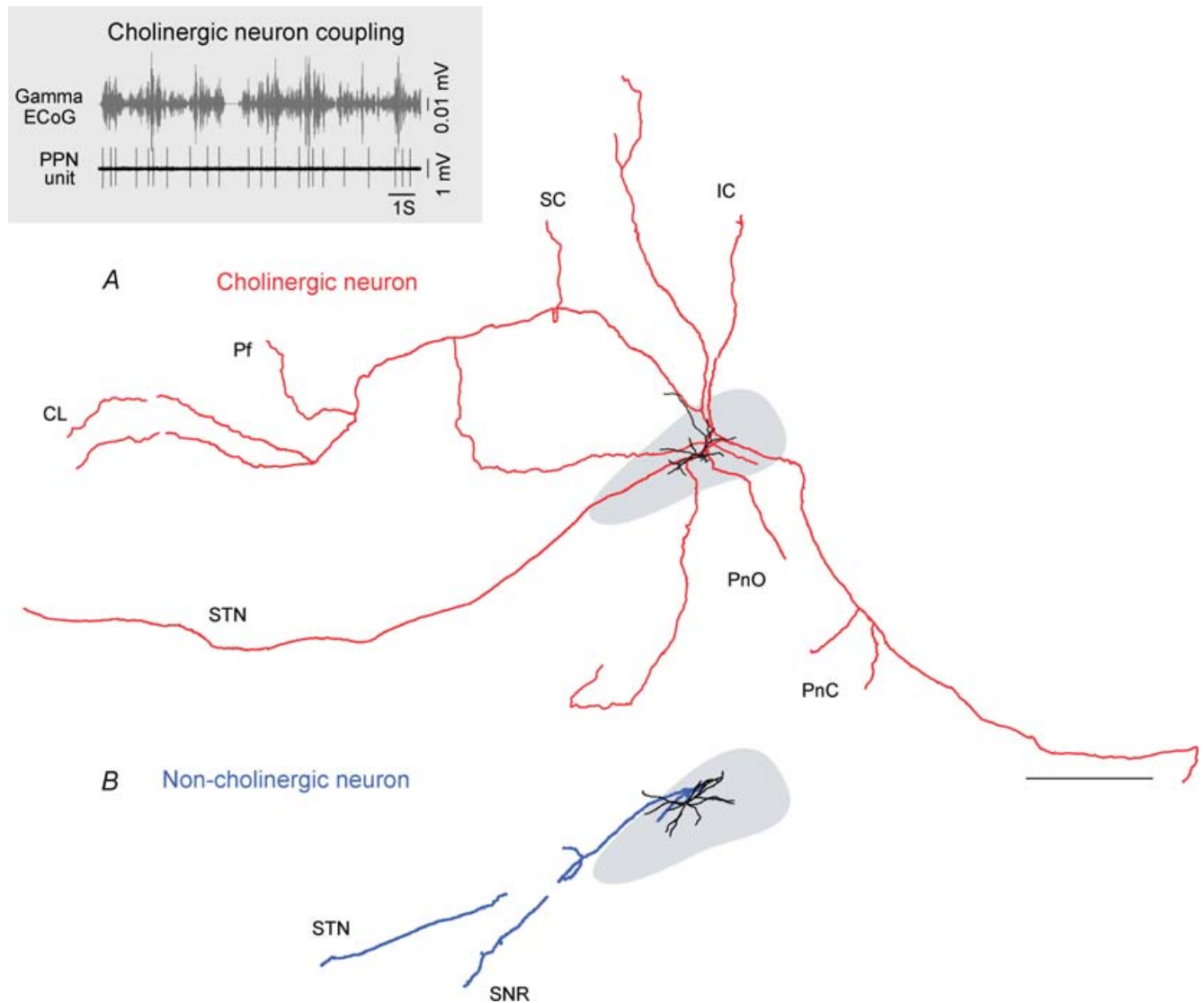


**Figure 5. Differences in connectivity between cholinergic and non-cholinergic neurons**

A, reconstruction of the cell body, dendrites (black) and axon (red) of an individual cholinergic PPN neuron. The PPN is shown in grey. All cholinergic neurons have both ascending and descending axonal projections to several brain areas, including the centrolateral (CL) and parafascicular (Pf) nuclei of the thalamus, superior and inferior colliculi (SC and IC), basal ganglia (STN, subthalamic nucleus) and lower brainstem (PnO, pontis oralis and PnC, pontis caudalis). This cholinergic neuron fired in time with increases in cortical gamma oscillations (30–50 Hz; grey) during slow-wave activity (inset). B, reconstruction of the cell body, dendrites (black) and axon (blue) of an individual non-cholinergic PPN neuron. Most non-cholinergic neurons were identified as projecting preferentially towards the basal ganglia (SNR, substantia nigra pars reticulata). Scale bar: 1 mm.

of some anaesthetics as a reliable model of natural slow-wave sleep arises from a considerable number of studies showing many comparable characteristics, such as the anatomical structures involved, the power and frequency of the oscillations, and the neurotransmitters implicated. Cortical slow oscillations present during urethane anaesthesia and natural sleep are similar (Steriade, 2006). Recordings of cortical activity in sleeping animals show that although natural slow oscillations are less stereotyped, i.e. have a slightly higher temporal and voltage variability than slow oscillations during anaesthesia, 1–2 Hz oscillations still dominate natural slow-wave sleep, indicating that such slow oscillations are not an artefact of urethane anaesthesia but rather reflect a basic physiological patterning (Urbain *et al.* 2000; Mahon *et al.* 2006). In fact, our results contribute to this idea by showing that, during urethane anaesthesia, a wake-inducing structure i.e. the PPN, is still responsive to spontaneous fluctuations in global brain states, and is able to respond to sensory stimuli (see Fig. 1).

Cholinergic PPN neurons fire spontaneously *in vitro* due to intrinsically generated, voltage-dependent oscillations. Thus, in the absence of any cortical influence, they show more rhythmic and more constant firing than non-cholinergic neurons due to calcium-dependent subthreshold membrane oscillations (below spike threshold) and high-threshold membrane oscillations, firing at a mean frequency of 9.6 Hz (Takakusaki & Kitai, 1997). Such firing properties are consistent with the type of activity required to maintain the constant levels of excitation of PPN targets during activated states in the intact brain. Our findings, however, show that cholinergic neuron firing pattern in the PPN during cortical SWA is in the form of oscillations at a frequency similar to the slow oscillations in the cortex ( $\sim 1$  Hz), suggesting that intrinsic membrane properties help maintain their activity during cortical slow oscillations along with rhythmic inputs arising through polysynaptic pathways

driven by the cortex. The cortical slow oscillation is generated through synchronous, rhythmic depolarizing (active component) and hyperpolarizing transitions in the membrane potentials of principal neurons (Steriade *et al.* 1993). Rhythmic discharges of corticofugal neurons effectively entrain subpopulations of neurons in subcortical structures, some of which have effective excitatory and inhibitory connections with the PPN, most notably the basal ganglia (Wilson & Kawaguchi, 1996; Magill *et al.* 2004; Mena-Segovia *et al.* 2004) and the basal forebrain (Semba *et al.* 1989; Saper *et al.* 2005). However, not all afferents to the PPN are entrained by the slow oscillations (e.g. substantia nigra pars reticulata; Magill *et al.* 2004). Nevertheless, an explanation for the rhythmic pattern observed in the slow-oscillatory cholinergic neurons could come from an episodic excitation and/or inhibition at a frequency near 1 Hz arising from afferent systems.

A key observation of the present study was the specificity of the discharge of the different neuronal subtypes identified in relation with the phases of the cortical slow oscillations, which was critical for their classification here. This, however, impedes the correlation of our data with those in previous reports where the global brain state was not monitored (Florio *et al.* 2007). Our data serve to highlight the pressing need to quantify ongoing brain states in future studies of PPN neurons. Thus, we observed that only ChATa neurons fired in phase with the gamma oscillations in the cortex. Conversely, 3 of 9 of the identified cholinergic neurons fired during the inactive component of the slow oscillations (ChATi) and had distinctive firing properties. These two types of cholinergic neurons may also represent the distinct cholinergic subtypes reported *in vitro* (Saitoh *et al.* 2003). In contrast to cholinergic neurons, we found that the firing of non-cholinergic neurons that are linked to cortical activity have a different phase relationship with the cortical SWA, and have a different pattern of connectivity. Thus, non-cholinergic

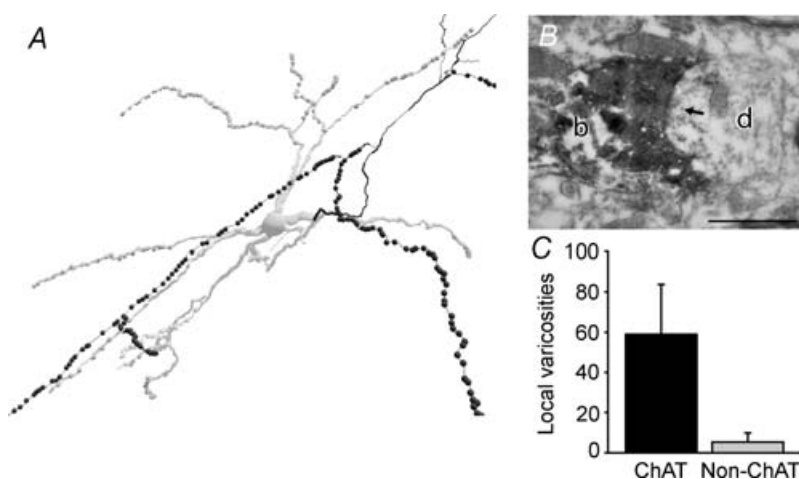


**Figure 6. Local connectivity in the PPN mediated by cholinergic neurons**

A, the same cholinergic neuron reconstruction shown in Fig. 5A at a higher magnification. Local axon collaterals (in black) of cholinergic neurons were typically studded with many varicosities (black dots). B, electron micrograph of one of the varicosities of the same neuron (b) establishing a synapse (arrow) with a dendrite (d) in PPN. C, cholinergic neurons ( $n = 10$ ) have a large number of local varicosities, compared to the scarce number of local varicosities from non-cholinergic neurons ( $n = 6$ ). Scale bar: 500 nm.

neurons have only ascending projections that in most of the cases travelled towards the basal ganglia. However, as is the case for cholinergic neurons, non-cholinergic neurons are also active during global slow oscillations and maintain a close relationship with the cortex, suggesting that they play a complementary role to cholinergic neurons in the activation of forebrain structures. The finding that the different neuronal subtypes fire in opposite phases during the slow oscillations in the cortex suggests an intrinsic

regulation of activity between the different subtypes and argues against global entrainment of the PPN by the cortex.

Our anatomical analyses also revealed key features of the connectivity of the PPN. We have discovered that individual cholinergic neurons in the PPN give rise to extensive axon collaterals innervating many regions of the brain, including key cortical afferent systems (most notably, the intralaminar thalamic nuclei), and give rise to local collaterals that form synapses within the PPN.

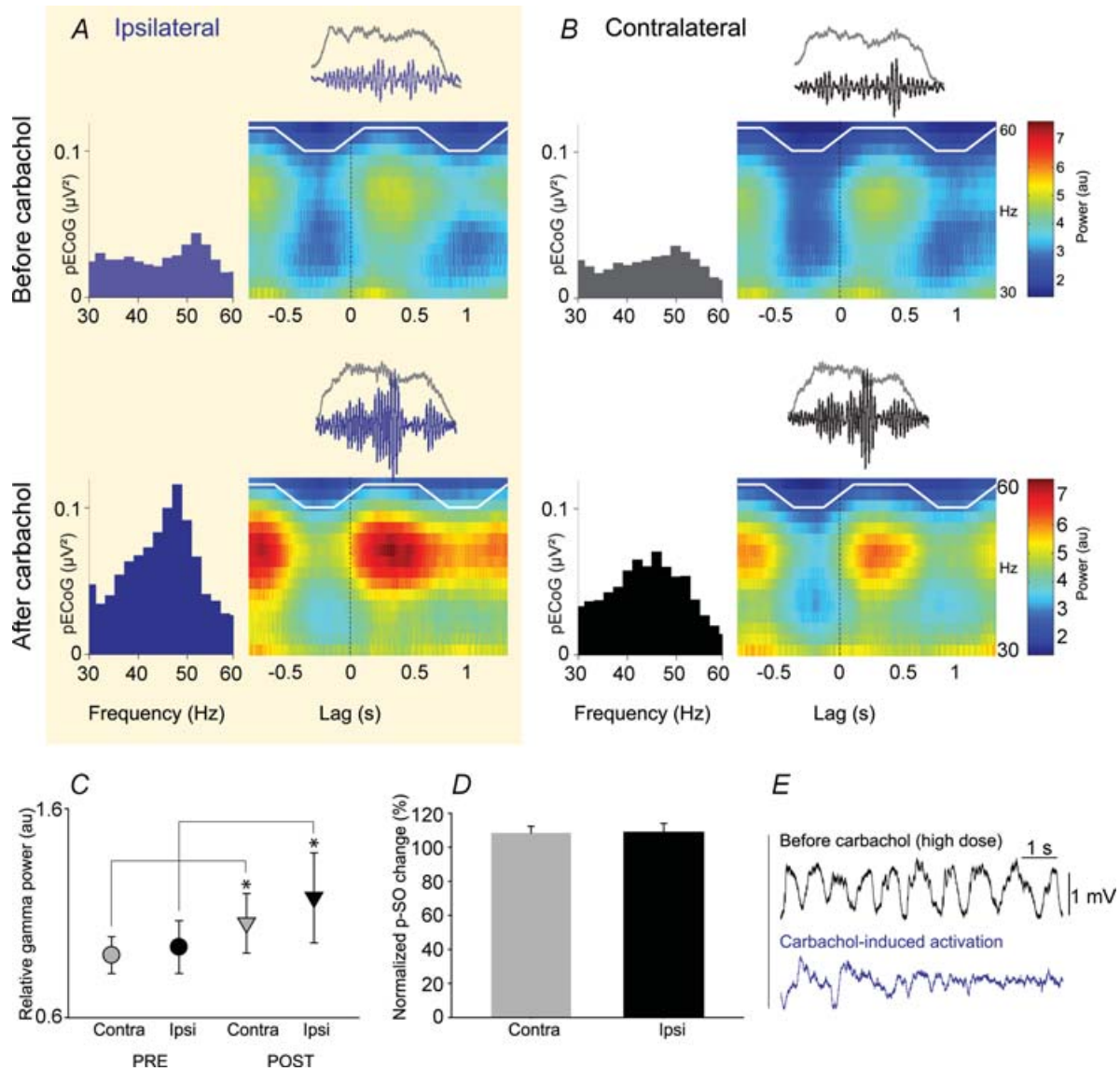


**Figure 7. Activation of acetylcholine receptors in the PPN enhances cortical gamma oscillations during slow-wave activity**

*A*, power spectra (left) and time-evolving spectrograms (right) of ECoGs highlighting typical gamma oscillations before and after injection of carbachol (2 nmol) into PPN in a single case. *B*, analysis of the side contralateral to the injection site in the same animal. *C*, carbachol administration in the PPN significantly increased the power of cortical gamma oscillations (30–50 Hz; mean  $\pm$  s.e.m.) ipsilateral and contralateral to the injection site ( $n = 5$ ,  $*P < 0.05$  (au, analog units)). *D*, carbachol injection did not produce a decrease in the power of the slow oscillations (p-SO). *E*, administration of a high dose of carbachol (100 nmol) into PPN obliterated cortical slow oscillations and produced an activated brain state.

They are thus in a position to influence, not only the activity of several other neuronal systems throughout the brain but, at the same time, their local neuronal network. This finding thus provides evidence against the common notion that the cholinergic component of the PPN operates purely as a relay nucleus, and is in good agreement with physiological evidence showing interconnections between PPN neurons (Garcia-Rill *et al.* 2007). We took advantage of this anatomical arrangement to determine the influence of cholinergic PPN neurons on cortical gamma oscillations; we mimicked the effect of activation of the cholinergic network within the PPN by the local application of carbachol and hence the stimulation of acetylcholine receptors. Indeed, recent evidence shows that carbachol is able to increase synchronization between electrically coupled PPN neurons (Garcia-Rill *et al.* 2007). Administration of a low dose of carbachol led to increases in nested gamma oscillations in the cortex but did not produce a sustained global activation, as was observed with higher doses by ourselves (Fig. 7E) and others (Kinney *et al.* 1998). Since stimulation of acetylcholine receptors in the PPN leads to increased firing of PPN neurons (Garcia-Rill *et al.* 2007; Good *et al.* 2007), the increases in nested gamma oscillations were presumably due to increasing the output of PPN neurons projecting to the thalamus and/or basal forebrain and thence the cortex. As cholinergic neurons were the only neuronal type in the PPN whose firing increases during the active component of the slow oscillations and therefore, cortical gamma oscillations, and because ChAT-immunoreactive axons terminals have been observed in contact with ChAT-immunoreactive dendrites in the PPN (Honda & Semba, 1995), it is likely that this effect was mediated by cholinergic neurons.

Overall our data support a novel hypothesis that cholinergic PPN neurons modulate cortical gamma oscillations during slow-wave sleep through local actions within the PPN and through their widespread projections to the forebrain. Nevertheless, cholinergic neurons in the PPN are unlikely to be the *only* source for this type of modulation, as intrinsic cortical circuits are able to generate gamma oscillations when in isolation (Llinas *et al.* 1991; Whittington *et al.* 1995). It is also possible that other elements from the so-called ARAS, known to induce wakefulness and inhibit sleep, contribute to the cortical activity during global slow wave activity. However, neither serotonin neurons in the dorsal raphe nucleus (Kocsis *et al.* 2006; Urbain *et al.* 2006), nor midbrain dopamine neurons (Dahan *et al.* 2007; M. Brown, personal communication), exhibit the same temporal relationship with cortical slow oscillations as we have shown here for brainstem cholinergic neurons. Furthermore, the activation of the noradrenergic neurons from the locus coeruleus has an inverse relationship to the absolute power of cortical gamma oscillations (Berridge & Foote, 1991). Rather, cholinergic neurons of the PPN might be contributing to

the proliferation of cortical gamma oscillations established through intrinsic (i.e. intracortical) mechanisms. Thus, PPN might provide a reinforcement of such oscillations at the thalamic level that will contribute to the integration of the subcortical information and the coherence between thalamocortical areas. In short, cholinergic neurons of the PPN should no longer be considered simply as part of a system capable of producing a strong cortical activation, but should instead be considered as part of a system that contributes to cortical activity across the whole of the sleep–wake cycle.

Slow-wave sleep, and particularly the cortical slow oscillation, is important for consolidating memory traces acquired during waking (Huber *et al.* 2004; Marshall *et al.* 2006). Gamma oscillations nested within slow oscillations could be involved in mentation, and indeed, might also support consolidation processes during sleep (Molle *et al.* 2004), thus complementing the roles of gamma oscillations in cognitive, motor and perceptual functions of the cortex during wakefulness (Maloney *et al.* 1997; Herrmann *et al.* 2004; Jensen *et al.* 2007). The functions supported by nested gamma oscillations during sleep are critically dependent on the gating of the underlying cortical ensembles, and our data provide direct evidence that cholinergic PPN neurons play key roles in this gating process.

## References

- Berridge CW & Foote SL (1991). Effects of locus coeruleus activation on electroencephalographic activity in neocortex and hippocampus. *J Neurosci* **11**, 3135–3145.
- Bevan MD, Booth PA, Eaton SA & Bolam JP (1998). Selective innervation of neostriatal interneurons by a subclass of neuron in the globus pallidus of the rat. *J Neurosci* **18**, 9438–9452.
- Buzsaki G & Draguhn A (2004). Neuronal oscillations in cortical networks. *Science* **304**, 1926–1929.
- Dahan L, Astier B, Vautrelle N, Urbain N, Kocsis B & Chouvet G (2007). Prominent burst firing of dopaminergic neurons in the ventral tegmental area during paradoxical sleep. *Neuropsychopharmacology* **32**, 1232–1241.
- Destexhe A, Hughes SW, Rudolph M & Crunelli V (2007). Are corticothalamic ‘up’ states fragments of wakefulness? *Trends Neurosci* **30**, 334–342.
- Donoghue JP & Wise SP (1982). The motor cortex of the rat: cytoarchitecture and microstimulation mapping. *J Comp Neurol* **212**, 76–88.
- Florio T, Scarnati E, Confalone G, Minchella D, Galati S, Stanzione P, Stefani A & Mazzone P (2007). High-frequency stimulation of the subthalamic nucleus modulates the activity of pedunculopontine neurons through direct activation of excitatory fibres as well as through indirect activation of inhibitory pallidal fibres in the rat. *Eur J Neurosci* **25**, 1174–1186.
- Garcia-Rill E (1991). The pedunculopontine nucleus. *Prog Neurobiol* **36**, 363–389.

- Garcia-Rill E, Heister DS, Ye M, Charlesworth A & Hayar A (2007). Electrical coupling: novel mechanism for sleep-wake control. *Sleep* **30**, 1405–1414.
- Good CH, Bay KD, Buchanan R, Skinner RD & Garcia-Rill E (2007). Muscarinic and nicotinic responses in the developing pedunclopontine nucleus (PPN). *Brain Res* **1129**, 147–155.
- Herrmann CS, Munk MH & Engel AK (2004). Cognitive functions of gamma-band activity: memory match and utilization. *Trends Cogn Sci* **8**, 347–355.
- Honda T & Semba K (1995). An ultrastructural study of cholinergic and non-cholinergic neurons in the laterodorsal and pedunclopontine tegmental nuclei in the rat. *Neuroscience* **68**, 837–853.
- Huber R, Ghilardi MF, Massimini M & Tononi G (2004). Local sleep and learning. *Nature* **430**, 78–81.
- Jensen O, Kaiser J & Lachaux JP (2007). Human gamma-frequency oscillations associated with attention and memory. *Trends Neurosci* **30**, 317–324.
- Kaneoke Y & Vitek JL (1996). Burst and oscillation as disparate neuronal properties. *J Neurosci Meth* **68**, 211–223.
- Kinney GG, Vogel GW & Feng P (1998). Brainstem carbachol injections in the urethane anesthetized rat produce hippocampal theta rhythm and cortical desynchronization: a comparison of pedunclopontine tegmental versus nucleus pontis oralis injections. *Brain Res* **809**, 307–313.
- Kita H & Armstrong W (1991). A biotin-containing compound N-(2-aminoethyl) biotinamide for intracellular labeling and neuronal tracing studies: comparison with biocytin. *J Neurosci Meth* **37**, 141–150.
- Kocsis B, Varga V, Dahan L & Sik A (2006). Serotonergic neuron diversity: identification of raphe neurons with discharges time-locked to the hippocampal theta rhythm. *Proc Natl Acad Sci U S A* **103**, 1059–1064.
- Lee MG, Hassani OK, Alonso A & Jones BE (2005). Cholinergic basal forebrain neurons burst with theta during waking and paradoxical sleep. *J Neurosci* **25**, 4365–4369.
- Llinas RR, Grace AA & Yarom Y (1991). In vitro neurons in mammalian cortical layer 4 exhibit intrinsic oscillatory activity in the 10- to 50-Hz frequency range. *Proc Natl Acad Sci U S A* **88**, 897–901.
- Magill PJ, Bolam JP & Bevan MD (2000). Relationship of activity in the subthalamic nucleus-globus pallidus network to cortical electroencephalogram. *J Neurosci* **20**, 820–833.
- Magill PJ, Sharott A, Bolam JP & Brown P (2004). Brain state-dependency of coherent oscillatory activity in the cerebral cortex and basal ganglia of the rat. *J Neurophysiol* **92**, 2122–2136.
- Mahon S, Vautrelle N, Pezard L, Slaght SJ, Deniau JM, Chouvet G & Charpier S (2006). Distinct patterns of striatal medium spiny neuron activity during the natural sleep-wake cycle. *J Neurosci* **26**, 12587–12595.
- Maloney KJ, Cape EG, Gotman J & Jones BE (1997). High-frequency gamma electroencephalogram activity in association with sleep-wake states and spontaneous behaviors in the rat. *Neuroscience* **76**, 541–555.
- Marshall L, Helgadottir H, Molle M & Born J (2006). Boosting slow oscillations during sleep potentiates memory. *Nature* **444**, 610–613.
- Mena-Segovia J, Bolam JP & Magill PJ (2004). Pedunclopontine nucleus and basal ganglia: distant relatives or part of the same family? *Trends Neurosci* **27**, 585–588.
- Molle M, Marshall L, Gais S & Born J (2004). Learning increases human electroencephalographic coherence during subsequent slow sleep oscillations. *Proc Natl Acad Sci U S A* **101**, 13963–13968.
- Moruzzi G & Magoun HW (1949). Brain stem reticular formation and activation of the electroencephalogram. *Electroencephalogr Clin Neurophysiol* **1**, 455–473.
- Munk MH, Roelfsema PR, Konig P, Engel AK & Singer W (1996). Role of reticular activation in the modulation of intracortical synchronization. *Science* **272**, 271–274.
- Pahapill PA & Lozano AM (2000). The pedunclopontine nucleus and Parkinson's disease. *Brain* **123**, 1767–1783.
- Paxinos G & Watson C (1986). *The Rat Brain in Stereotaxic Coordinates*. Academic Press, San Diego.
- Pinault D (1996). A novel single-cell staining procedure performed in vivo under electrophysiological control: morpho-functional features of juxtacellularly labeled thalamic cells and other central neurons with biocytin or Neurobiotin. *J Neurosci Meth* **65**, 113–136.
- Rudolph M, Pospischil M, Timofeev I & Destexhe A (2007). Inhibition determines membrane potential dynamics and controls action potential generation in awake and sleeping cat cortex. *J Neurosci* **27**, 5280–5290.
- Saitoh K, Hattori S, Song WJ, Isa T & Takakusaki K (2003). Nigral GABAergic inhibition upon cholinergic neurons in the rat pedunclopontine tegmental nucleus. *Eur J Neurosci* **18**, 879–886.
- Sanchez-Vives MV & McCormick DA (2000). Cellular and network mechanisms of rhythmic recurrent activity in neocortex. *Nat Neurosci* **3**, 1027–1034.
- Saper CB, Scammell TE & Lu J (2005). Hypothalamic regulation of sleep and circadian rhythms. *Nature* **437**, 1257–1263.
- Semba K, Reiner PB, McGeer EG & Fibiger HC (1989). Brainstem projecting neurons in the rat basal forebrain: Neurochemical, topographical, and physiological distinctions from cortically projecting cholinergic neurons. *Brain Res Bull* **22**, 501–509.
- Steriade M (2000). Corticothalamic resonance, states of vigilance and mentation. *Neuroscience* **101**, 243–276.
- Steriade M (2006). Grouping of brain rhythms in corticothalamic systems. *Neuroscience* **137**, 1087–1106.
- Steriade M, Amzica F & Contreras D (1996). Synchronization of fast (30–40 Hz) spontaneous cortical rhythms during brain activation. *J Neurosci* **16**, 392–417.
- Steriade M, Amzica F & Nunez A (1993). Cholinergic and noradrenergic modulation of the slow (approximately 0.3 Hz) oscillation in neocortical cells. *J Neurophysiol* **70**, 1385–1400.
- Steriade M, Datta S, Pare D, Oakson G & Curro Dossi RC (1990). Neuronal activities in brain-stem cholinergic nuclei related to tonic activation processes in thalamocortical systems. *J Neurosci* **10**, 2541–2559.
- Steriade M, Dossi RC, Pare D & Oakson G (1991). Fast oscillations (20–40 Hz) in thalamocortical systems and their potentiation by mesopontine cholinergic nuclei in the cat. *Proc Natl Acad Sci U S A* **88**, 4396–4400.

- Takakusaki K & Kitai ST (1997). Ionic mechanisms involved in the spontaneous firing of tegmental pedunculo-pontine nucleus neurons of the rat. *Neuroscience* **78**, 771–794.
- Ungless MA, Magill PJ & Bolam JP (2004). Uniform inhibition of dopamine neurons in the ventral tegmental area by aversive stimuli. *Science* **303**, 2040–2042.
- Urbain N, Creamer K & Debonnel G (2006). Electrophysiological diversity of the dorsal raphe cells across the sleep–wake cycle of the rat. *J Physiol* **573**, 679–695.
- Urbain N, Gervasoni D, Souliere F, Lobo L, Rentero N, Windels F, Astier B, Savasta M, Fort P, Renaud B, Luppi PH & Chouvet G (2000). Unrelated course of subthalamic nucleus and globus pallidus neuronal activities across vigilance states in the rat. *Eur J Neurosci* **12**, 3361–3374.
- Whittington MA, Traub RD & Jefferys JG (1995). Synchronized oscillations in interneuron networks driven by metabotropic glutamate receptor activation. *Nature* **373**, 612–615.
- Wilson CJ & Kawaguchi Y (1996). The origins of two-state spontaneous membrane potential fluctuations of neostriatal spiny neurons. *J Neurosci* **16**, 2397–2410.

- Winn P (2006). How best to consider the structure and function of the pedunculo-pontine tegmental nucleus: evidence from animal studies. *J Neurol Sci* **248**, 234–250.

### Acknowledgements

We thank J. Creso and Dr L. Marton for their assistance with data analysis, and B. Micklem, E. Norman, K. Whitworth and C. Francis for technical assistance. This work was funded by the Medical Research Council UK, the Parkinson's Disease Society of the UK (grant no. 4049) and the Parkinson's Disease Foundation. J.M.S. was partly supported by The International Human Frontier Science Program Organization. H.M.S. was in receipt of an MRC studentship.

### Author's present address

H.M. Sims: Department of Neurobiology, Yale University School of Medicine, 333 Cedar Street, SHM C-316, New Haven, CT 06510, USA.